

## Finite Element Analysis of the Inclined Subsurface Cracks in a Homogeneous Body Under a Moving Compressive Load

Kyung-Sick Lee<sup>†</sup> and Gyu-Sung Chung

School of Mechanical and Automotive Engineering, University of Ulsan, San-29 Mugeo-2 Dong, Namgu, Ulsan 680-749, Korea

**Abstract:** The inclined subsurface cracks in a homogeneous body subjected to a moving compressive load is analyzed with the finite element method (FEM) considering friction on the crack surface. The stress intensity factors for the inclined subsurface cracks are evaluated numerically for various cases such as different inclined angles and changes in the coefficient of friction. The effects of the inclined angle and the coefficient of friction on the stress intensity factor are discussed. The difference between the behaviors of the parallel subsurface crack and those of the inclined subsurface crack is also examined.

**Key words:** Inclined subsurface crack, moving load, FEM, stress intensity factor

### Introduction

A great number of papers concerning propagation of the subsurface cracks in an elastically deforming homogeneous material have been published since Suh [1] introduced the delamination theory of wear. Fleming and Suh [2] obtained the stress intensity factor for the subsurface crack under a moving compressive load without considering friction on the crack surface. Rosenfield [3], Hills and Ashelby [4] and Keer and coworkers [5,6], on the other hand, considered friction on the crack surface and obtained the stress intensity factors for the subsurface crack under a moving compressive load [3,4] or Hertzian contact load [5,6]. However, they did not take account of the loading path dependence caused by frictional contact on the crack surface. Hearle and Johnson [7] and Sheppard *et al.* [8,9] have obtained the stress intensity factors for the subsurface cracks considering the loading path dependence as well as friction on the crack surface. Recently, Lee *et al.* [10] obtained stress intensity factors for the subsurface cracks not only in a homogenous material but also on the interface between dissimilar materials.

All researches mentioned above analyzed the subsurface crack which is laid parallel to the surface. In the present work, the inclined subsurface cracks in a homogeneous body subjected to a moving compressive load are analyzed by the finite element method (FEM), considering friction on the crack surface. The stress intensity factors for the inclined subsurface cracks are calculated for various cases such as different angles of inclination, changes in the coefficients of friction on the crack surface and changes in the coefficients of friction on the surface. The effects of the inclined angle and the coefficients of friction on the behavior of the subsurface crack are discussed, and the difference between the behaviors of the parallel

subsurface crack and those of the inclined subsurface crack is also examined.

### Finite element analysis

#### Description of the problem

The delamination wear is interpreted as a process of gradual propagation of the subsurface crack due to the external load acting on the surface repeatedly. Most of the previous studies related to the delamination wear analyzed the subsurface cracks which are parallel to the surface to investigate the propagation of the crack. But the subsurface crack, which is the initial defect under the surface, can be oriented randomly. So it is necessary to analyze the inclined subsurface crack in order to understand the delamination wear process better. Figure 1 depicts the geometry of the inclined subsurface crack in a homogeneous material subjected to a moving compressive

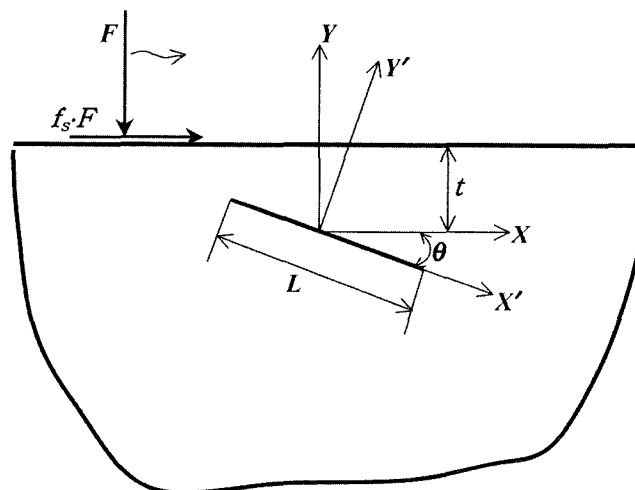


Fig. 1. Geometry of the inclined subsurface crack in a homogeneous body subjected to a moving load.

<sup>†</sup>Corresponding author; Tel: +82-52-259-2134, Fax: +82-52-259-1680  
E-mail: kslee@mail.ulsan.ac.kr

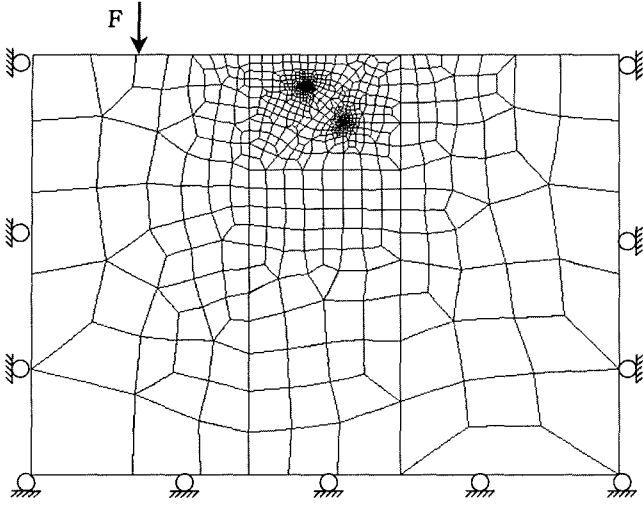


Fig. 2. Finite element mesh for the inclined subsurface crack for the case of  $\theta = 45^\circ$ .

load. In this figure,  $L$  denotes the length of the crack,  $t$  is the depth of the crack from the free surface and  $\theta$  is the angle of inclination. In the present work, the stress intensity factors at both crack tips are evaluated numerically for various cases such as different angles of inclination, changes in the coefficients of friction on the crack surface ( $f_c$ ) and changes in the coefficients of friction on the surface ( $f_s$ ).

The following assumptions are employed in the present work.

- (1) A state of plane strain is assumed within the framework of the infinitesimal deformation theory.
- (2) The material is isotropic and linearly elastic.
- (3) Coulombs friction law holds on the contacting surfaces.
- (4) A compressive load  $F$  moves along the  $X$  axis very slowly so that any inertia effect can be neglected.

Figure 2 shows one of the finite element meshes used in the present work. The commercial pre-processor (I-deas) were employed to generate the mesh automatically. The eight-noded isoparametric elements were used and both the quarter-point crack tip element [11] and the transition element [12] were used to simulate the singularity at the crack tip. The angles of inclination considered in the present work are  $0^\circ$ ,  $15^\circ$ ,  $30^\circ$ ,  $45^\circ$ ,  $60^\circ$  and  $75^\circ$ . In each case of the inclined angle, the coefficients of the friction on the crack surface ( $f_c$ ) and the coefficients of the friction on the surface ( $f_s$ ) are set to 0.1, 0.3 and 0.5. The magnitude of the compressive line load  $F$  is 1 N/mm and the ratio of the crack length  $L$  to the depth of the crack  $t$  equals to 1. The finite element program used in the present work is the program which was used in the previous work of Lee [10]. The accuracy and the usefulness of this finite element program was already verified in that work of Lee [10], and the solution method for the frictional contact problem and the treatment of the moving load were also explained.

### Computation of the stress intensity factor

Two methods are generally used to compute the stress intensity factor by the finite element method. One is the  $J$ -integral

method and the other is the crack surface displacement method. In case of the present work, there exists a non-conservative frictional traction on the crack surface. Hence the  $J$ -integral method seems to be inappropriate since the path independence of the  $J$ -integral does not hold any more. Thus, in the present work, the stress intensity factors are obtained from the crack surface displacements in the following manner.

The crack surface displacements at a distance  $r$  from a crack tip are related to the stress intensity factors such that

$$\delta_y + i\delta_x = 8 \frac{1-\nu^2}{E} (K_I + iK_{II}) \left( \frac{r}{2\pi} \right)^{1/2} \quad (1)$$

where  $\delta_x$  and  $\delta_y$  are given by the following equations

$$\delta_x = u_x(-r, 0^+) - u_x(-r, 0^-) \quad (2)$$

$$\delta_y = u_y(-r, 0^+) - u_y(-r, 0^-)$$

and  $K_I$  and  $K_{II}$  are stress intensity factor of mode I and mode II respectively. In equation (2),  $0^+$  denotes the upper crack face and  $0^-$  denotes the lower crack face, and  $x$  denotes the axis parallel to the crack surfaces and  $y$  denotes the axis perpendicular to the crack surface. In the present work, the stress intensity factors are computed from the displacement of a corner node (at  $r = 0.2$  mm) of the crack tip element.

## Results and discussion

### Variation of the stress intensity factor with load position

Fig. 3 shows the variation of the non-dimensionalized stress intensity factor  $K^*$  with respect to the load position for various cases of  $\theta$ . The non-dimensionalized stress intensity factor  $K^*$  is defined by

$$K^* = \frac{K\pi t^{1/2}}{2F} \quad (3)$$

where  $F$  is the moving load and  $t$  is the depth of the crack. In the present work, the positive value of  $K_{II}^*$  means that the upper crack face moves right relative to the lower crack face (forward slip), and the negative value of  $K_{II}^*$  means that the upper crack face moves left relative to the lower crack face (backward slip). In case of horizontal subsurface crack ( $\theta = 0^\circ$ ), it can be seen from Fig. 3(a) that the upper crack face begins to slip forward and the stress intensity factor increases as the load approach the crack. After  $K_{II}^*$  obtains its maximum value ( $K_{IImax}^*$ ), the upper crack face begins to slip backward and the stress intensity factor decrease rapidly and  $K_{II}^*$  obtains its minimum value ( $K_{IImin}^*$ ). It can also be known from Fig. 3(a) that the magnitude of  $K_{IImax}^*$  is almost the same as that of  $K_{IImin}^*$  at both crack tips and the mode I stress intensity factor  $K_I$  has the value of nearly 0 throughout the loading path. In cases of the inclined subsurface cracks whose angle of inclination are  $15^\circ$  and  $30^\circ$ , the variation of the stress intensity factor with load position is similar to that for the case of horizontal subsurface crack, but the magnitude of  $K_{IImin}^*$  is smaller than that for the case of horizontal subsurface crack.

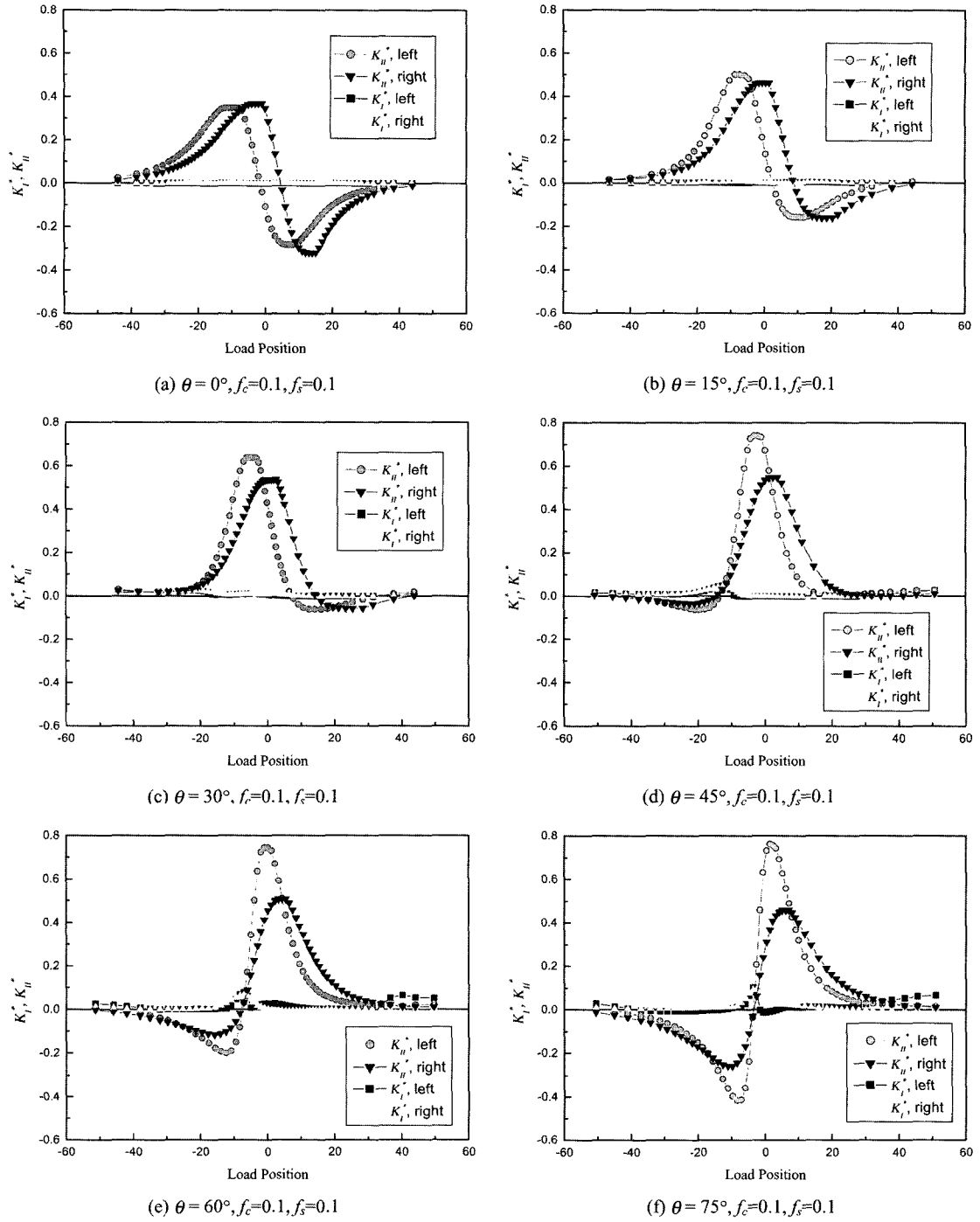


**Fig. 3. Variation of the non-dimensionalized stress intensity factors with load position.**

In cases of  $\theta = 45^\circ, 60^\circ$  and  $75^\circ$ , the variation of the stress intensity factor with load position is different from that for the cases of  $\theta = 0^\circ, 15^\circ$  and  $30^\circ$ . It can be found from Fig. 3(d)-3(f) that the upper crack face slips backward first and then slips forward, and that the magnitude of  $K_{II}^{*max}$  and  $K_{II}^{*min}$  increase as the angle of inclination increases but the increasing rate of  $K_{II}^{*max}$  is less than that of  $K_{II}^{*min}$ . It can also be noticed that the mode I stress intensity factor  $K_I^*$  has somewhat larger values, and  $K_I^*$  gets its maximum value when the load comes to the position where  $K_{II}^*$  becomes zero and this position is near the

point where the extension of crack axis ( $X'$ ) meets the free surface. This can be explained as follows. According to the Flamant solution for the concentrated force on a straight boundary [13], when the force acts at point where the extension of crack axis ( $X'$ ) and the surface intersect, the only stress component that exist at the crack tip is the radial component ( $\sigma_r$ ).  $\sigma_y$  and  $\tau_{xy}$  are zero. So the inclined subsurface crack is compressed along the crack axis ( $X'$ ) and consequently the crack is deformed into the elliptical shape. Because there is no shear stress component, the relative displacement between

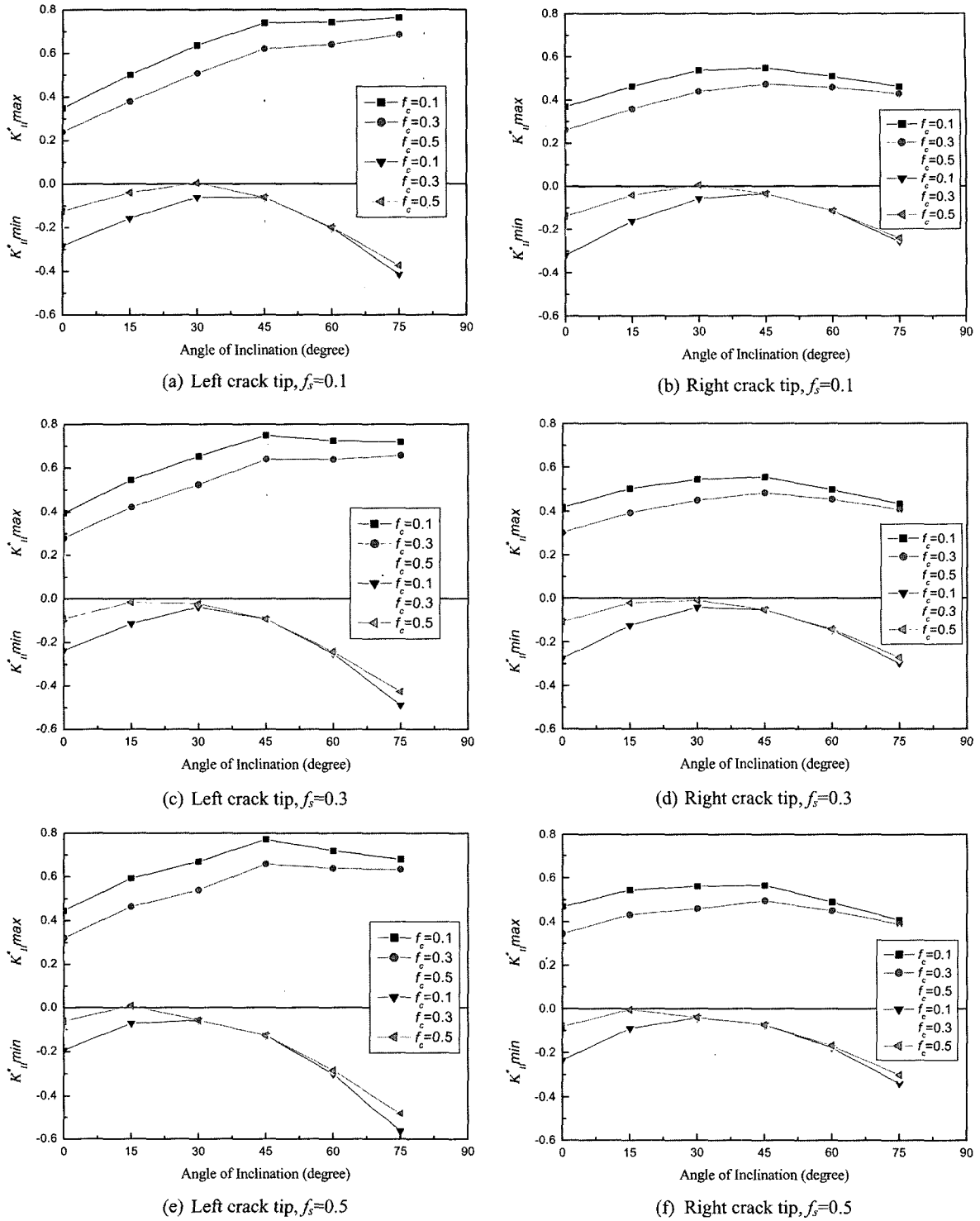


Fig. 4. Maximum and minimum values of the non-dimensionalized stress intensity factors as a function of the angle of inclination.

the upper the lower crack surfaces is zero so that the mode II stress intensity factor is zero. Similarly the value of the mode I stress intensity factor  $K_I^*$ , becomes larger as the angle of inclination increases.

#### The maximum and minimum values of $K_{II}^*$

The maximum and minimum values of  $K_{II}^*$  at crack tips are shown in Fig. 4 as a function of the angle of inclination  $\theta$  for

various coefficients of friction on the crack surface and surface. At both crack tips,  $K_{II,max}^*$  increases as the angle of inclination increases up to  $45^\circ$ . For the case of  $\theta = 60^\circ$  and  $75^\circ$ ,  $K_{II,max}^*$  has a little smaller values than that for the case of  $\theta = 45^\circ$  when the coefficient of friction on the surface  $f_s$  becomes large. The magnitude of  $K_{II,max}^*$  at the left crack tip is larger than that at the right crack tip except the case of  $\theta = 0^\circ$ . As the coefficient of friction on the crack surface  $f_c$  increases

**Table 1.**  $K_{II\max}^*$  and  $K_{II\min}^*$  values at both crack tips of the inclined subsurface cracks under a moving compressive load

$\theta$	$f_s$	$f_c$	Left crack tip		Right crack tip	
			$K_{II\max}^*$	$K_{II\min}^*$	$K_{II\max}^*$	$K_{II\min}^*$
0°	0.1	0.1	0.348	-0.283	0.368	-0.319
		0.3	0.240	-0.189	0.261	-0.214
		0.5	0.162	-0.124	0.178	-0.138
	0.3	0.1	0.395	-0.237	0.417	-0.275
		0.3	0.279	-0.150	0.302	-0.177
		0.5	0.194	-0.092	0.212	-0.108
	0.5	0.1	0.445	-0.194	0.468	-0.234
		0.3	0.320	-0.112	0.345	-0.143
		0.5	0.227	-0.061	0.247	-0.081
15°	0.1	0.1	0.501	-0.157	0.463	-0.161
		0.3	0.379	-0.085	0.358	-0.088
		0.5	0.287	-0.040	0.272	-0.041
	0.3	0.1	0.546	-0.113	0.502	-0.124
		0.3	0.422	-0.051	0.393	-0.061
		0.5	0.326	-0.016	0.304	-0.022
	0.5	0.1	0.591	-0.071	0.543	-0.090
		0.3	0.464	-0.019	0.431	-0.035
		0.5	0.365	0.009	0.337	-0.005
30°	0.1	0.1	0.638	-0.061	0.536	-0.056
		0.3	0.509	-0.017	0.439	-0.015
		0.5	0.408	0.005	0.356	0.005
	0.3	0.1	0.654	-0.037	0.544	-0.040
		0.3	0.524	-0.003	0.448	-0.006
		0.5	0.421	0.011	0.364	0.007
	0.5	0.1	0.670	-0.014	0.559	-0.026
		0.3	0.539	0.011	0.459	-0.001
		0.5	0.434	0.024	0.373	0.007

the magnitude of  $K_{II\max}^*$  decreases, and this is because the relative motion of the crack surfaces is prohibited by the action of friction. In the cases where the angle of inclination  $\theta$  is smaller than  $60^\circ$ , as the coefficient of friction on the surface  $f_s$  increases the magnitude of  $K_{II\max}^*$  increases, and in the cases of  $\theta = 60^\circ$  and  $75^\circ$  the magnitude of  $K_{II\max}^*$  becomes smaller as  $f_s$  increases. This can be explained as follows. As the tangential traction on the surface increases, the angle between the displacement of the upper crack surface and the axis of crack becomes larger and the component of the displacement along the crack axis decreases.

The variation of  $K_{II\min}^*$  with the angle of inclination differs from that of  $K_{II\max}^*$ . As the angle of inclination  $\theta$  increases, the magnitude of  $K_{II\min}^*$  decreases first and takes its minimum at  $\theta = 15^\circ$  or  $30^\circ$  and then increases continuously. For the case of  $\theta$  less than  $30^\circ$ , the upper crack surface slips forward first and then slips backward, and the back-slip takes place due to the lateral displacement of the body under a load when the load is on the right side of the crack tip. So at both crack tips for the cases of  $\theta = 0^\circ$ ,  $15^\circ$  and  $30^\circ$ , the magnitude of  $K_{II\min}^*$  decreases as  $\theta$  increases, and increases as  $f_s$  and  $f_c$  decreases. As mentioned in the section 3.1, the crack behavior for the cases

of  $\theta = 45^\circ$ ,  $60^\circ$  and  $75^\circ$  is different from that for the case of  $\theta = 0^\circ$ ,  $15^\circ$  and  $30^\circ$ , and the upper crack surface slips backward first and  $K_{II}^*$  takes the minimum value and the slips forward and also  $K_{II}^*$  takes somewhat large value. For the cases of  $\theta = 45^\circ$ ,  $60^\circ$  and  $75^\circ$ , the magnitude of  $K_{II\min}^*$  at both crack tips increases as  $\theta$  and  $f_s$  increases, and the coefficient of friction on the crack surface  $f_c$  does not have effect on  $K_{II\min}^*$  except for the case of  $\theta = 75^\circ$  because the crack surfaces are not in contact when  $K_{II}^*$  has the positive values.

The numerical values of  $K_{II\max}^*$  and  $K_{II\min}^*$  for the various cases of inclined subsurface cracks are given in Table 1.

## Conclusions

The inclined subsurface cracks subjected to a moving compressive load were analyzed with the finite element method considering the friction on the crack surface. By investigating the variation of the stress intensity factor with load position at both crack tips and the effects of the angle of inclination  $\theta$ , the coefficient of friction on the crack surface  $f_c$  and the coefficient of friction on the surface  $f_s$ , the following conclusions were obtained.

Table 1. (continued)

$\theta$	$f_s$	$f_c$	Left crack tip		Right crack tip	
			$K^*_{II\ max}$	$K^*_{II\ min}$	$K^*_{II\ max}$	$K^*_{II\ min}$
45°	0.1	0.1	0.740	-0.063	0.548	-0.034
		0.3	0.622	-0.063	0.472	-0.034
		0.5	0.523	-0.063	0.404	-0.034
	0.3	0.1	0.750	-0.094	0.555	-0.054
		0.3	0.640	-0.094	0.483	-0.054
		0.5	0.546	-0.094	0.417	-0.054
	0.5	0.1	0.771	-0.126	0.564	-0.074
		0.3	0.658	-0.126	0.496	-0.074
		0.5	0.570	-0.126	0.433	-0.074
60°	0.1	0.1	0.744	-0.201	0.508	-0.116
		0.3	0.641	-0.200	0.457	-0.115
		0.5	0.560	-0.198	0.409	-0.114
	0.3	0.1	0.725	-0.251	0.497	-0.146
		0.3	0.640	-0.246	0.452	-0.144
		0.5	0.560	-0.242	0.409	-0.142
	0.5	0.1	0.718	-0.303	0.488	-0.177
		0.3	0.638	-0.293	0.449	-0.173
		0.5	0.561	-0.285	0.410	-0.169
75°	0.1	0.1	0.763	-0.415	0.460	-0.256
		0.3	0.685	-0.393	0.428	-0.246
		0.5	0.629	-0.375	0.396	-0.239
	0.3	0.1	0.719	-0.489	0.432	-0.298
		0.3	0.657	-0.454	0.407	-0.283
		0.5	0.608	-0.427	0.381	-0.271
	0.5	0.1	0.679	-0.562	0.407	-0.341
		0.3	0.633	-0.520	0.388	-0.321
		0.5	0.587	-0.481	0.367	-0.302

(1) In the cases of the subsurface crack whose angle of inclination  $\theta$  equals 45° or greater, the upper crack surface slips backward first and  $K^*_{II}$  takes its minimum value and then it slips forward and  $K^*_{II}$  takes its maximum value. And  $K^*_I$  takes somewhat large values comparing with that for the case of horizontal subsurface crack.

(2) In the cases of the subsurface crack whose angle of inclination  $\theta$  equals 45° or less, the magnitude of  $K^*_{II\ max}$  increases as  $\theta$  and  $f_s$  increase. For the cases of  $\theta = 60^\circ$  and  $75^\circ$ , the magnitude of  $K^*_{II\ max}$  decreases as  $\theta$  and  $f_s$  increase. As the coefficient of friction on the crack surface  $f_c$  increases, the magnitude of  $K^*_{II\ max}$  decreases for all cases of  $\theta$  and  $f_s$ .

(3) As the angle of inclination  $\theta$  increases, the magnitude of  $K^*_{II\ min}$  decreases first and takes its minimum at  $\theta = 15^\circ$  or  $30^\circ$  and then increases continuously. For the cases of  $\theta = 0^\circ$ ,  $15^\circ$  and  $30^\circ$ , the magnitude of  $K^*_{II\ min}$  decreases as  $\theta$  increases, and increases as  $f_s$  and  $f_c$  decreases. For the cases of  $\theta = 45^\circ$ ,  $60^\circ$  and  $75^\circ$ , the magnitude of  $K^*_{II\ min}$  increases as  $\theta$  and  $f_s$  increases, and the coefficient of friction on the crack surface  $f_c$  does not have effect on  $K^*_{II\ min}$  except for the case of  $\theta = 75^\circ$ .

### Acknowledgment

This work was supported by the Korea Science and Engineering Foundation (KOSEF) through the Research Center for Machine Parts and Materials Processing (ReMM) at University of Ulsan.

### References

1. N. P. Suh, "The delamination theory of wear," *Wear*, Vol. 20, pp. 111-124, 1973.
2. J. R. Flemming, N. P. Suh, "Mechanics of crack propagation in delamination wear," *Wear*, Vol. 44, pp. 39-56, 1977.
3. A. R. Rosenfield, "A fracture mechanics approach to wear," *Wear*, Vol. 61, pp. 125-132, 1980.
4. D. A. Hills, D. W. Ashelby, "On the application of fracture mechanics to wear," *Wear*, Vol. 54, pp. 321-330, 1979.
5. L. M. Keer, M. D. Bryant and G. K. Haritos, "Subsurface and Surface Cracking Due to Hertzian Contact," *ASME J. Lubr. Tech.*, Vol. 104, pp. 347-351, 1982.
6. L. M. Keer, M. D. Bryant, "A pitting model for rolling

- contact fatigue," *J. Lubr. Tech.*, Vol. 105, pp. 198-205, 1983.
7. A. D. Hearle, K. L. Johnson, "Mode II Stress Intensity Factors for a Crack Parallel to the Surface of an Elastic Half Space Subjected to a Moving Point Load," *J. Mech. Phys. Solids*, Vol. 33, pp. 61-81, 1985.
  8. S. Sheppard, J. R. Barber and M. Comninou, "Short Subsurface Cracks Under Conditions of Slip and Stick Caused by a Moving Compressive Load," *ASME J. Appl. Mech.*, Vol. 52, pp. 811-817, 1985.
  9. S. Sheppard, J. R. Barber and M. Comninou, "Subsurface Cracks Under Conditions of Slip, Stick, Separation Caused by a Moving Compressive Load," *ASME J. Appl. Mech.*, Vol. 54, pp. 393-398, 1987.
  10. K. S. Lee, J. T. Tinn and Y. Y. Earmme, "Finite element analysis of a subsurface crack on the interface of a coated material under a moving compressive load," *Wear*, Vol. 155, pp. 117-136, 1992.
  11. R. S. Barsoum, "On the use of isoparametric finite elements in linear fracture mechanics," *Int. J. Numer. Methods Eng.*, Vol. 10, pp. 25-37, 1976.
  12. P. P. Lynn, A. R. Ingraffea, "Transition elements to be used with quarter-point crack-tip elements," *Int. J. Numer. Methods Eng.*, Vol. 12, pp. 1031-1036, 1978.
  13. L. W. Malvern, *Introduction to the Mechanics of a Continuous Medium*, Chap. 8, p. 539, Prentice hall, Eaglewood Cliffs, 1969.